J. Mol. Biol. (1995) **254**, 544–551

JMB

COMMUNICATION

A Novel Basis for Capsid Stabilization by Antiviral Compounds

Donald K. Phelps and Carol Beth Post*

Department of Medicinal Chemistry, Purdue University, West Lafayette IN 47907, USA

**Corresponding author*

Picornaviruses are inactivated by a family of hydrophobic drugs that bind at an internal site in the viral capsid and inhibit viral uncoating. A basis for the capsid stabilization previously unrecognized is revealed by molecular dynamics simulations of the antiviral drug WIN52084s bound to a hydrophobic pocket of solvated human rhinovirus 14. Isothermal compressibilities of the complex and human rhinovirus 14 without the antiviral drug calculated from density fluctuations show that the presence of WIN52084s increases the compressibility of the viral capsid near the antiviral drug. This counterintuitive result is understandable on the basis of the empirical evidence of thermal melting temperatures and protein-folding entropies of globular proteins. Based on this evidence, we propose that a larger compressibility from drug binding confers greater thermal stability to capsid proteins by increasing the conformational entropy of capsids, thereby diminishing the entropy gain with uncoating. We suggest that compressibility is fundamental to the structural integrity of viral capsids and that examination of compressibility and antiviral activity will provide insights into the disassembly process.

Keywords: antiviral; protein compressibility; molecular dynamics; rhinovirus; thermal stability

Mechanisms of antiviral activity are of considerable interest not only for developing a rationale for designing new antiviral drugs, but also as a means to understand the viral life cycle. A family of hydrophobic drugs has been developed against human rhinovirus (HRV), the causative agent of the common cold. These drugs, including the subject of this study WIN52084s (Figure 1A), bind in an internal site in the viral capsid that is naturally occupied by water molecules (Rossmann *et al*., 1985) or a long-chain molecule of unknown identity (Filman *et al*., 1989; Rossmann, 1994), and can inhibit viral uncoating, resulting in the disruption of the viral life cycle (Pevear *et al*., 1989).† The WIN compounds inhibit uncoating of HRV at high temperatures (Bibler-Muckelbauer *et al*., 1994) and at low pH (Heinz *et al*., 1990). The latter may be significant to antiviral activity because of the low pH environment of the endosome enclosing the virus in the host cell prior to uncoating. While studies of WIN-type compounds show that these drugs stabilize the capsid, the mechanism of stabilization is not known.

As a first step toward understanding the basis of this stabilization, we have investigated by computer simulation methods the dynamics of the pocket region of HRV14 when the pocket is occupied either by water or by WIN52084s. HRV14 is the subject of this study because of the availability of both unligated (Rossmann *et al*., 1985) and drug-bound (Badger *et al*., 1988) atomic resolution virus structures. A comparison of compressibility estimated from density fluctuations in the absence or presence of WIN52084s suggests a previously unrecognized basis for structural stabilization by the antiviral compound.

HRV14 is an icosahedral virus comprising 60 protomers of four polypeptides (VP1, VP2, VP3 and VP4) in the mature virion (Figure 2A). Crystallographic studies revealed a deep groove, or

Abbreviations used: HRV, human rhinovirus; SBMD, stochastic boundary molecular dynamics; HRP, horseradish peroxidase.

† Antipicorna-viral compounds in some cases also prevent intracellular adhesion molecules on the surface of host epithelial cells from recognizing binding sites on the viral protein surface (Pevear *et al*., 1989). Although both types of inhibition are known, the analysis described here relates only to inhibition of uncoating.

0022–2836/95/490544–08 $12.00/0

''canyon'', in the surface of the capsid, which encircles each viral 5-fold axis. The drug-binding pocket is located in VP1 below the groove, toward the interior of the capsid, such that a WIN compound occupying the pocket lies partially within the β-sandwich characteristic of most viral capsid proteins (Figure 1B). With one pocket per protomer, there are 60 drug-binding sites per virion. Similar pockets are seen in other picornaviruses, such as poliovirus (Filman *et al*., 1989), suggesting a functional role for the pocket in viral replication (Smith *et al*., 1986; Heinz *et al*., 1989; Grant *et al*., 1994). WIN binding produces conformational changes of as much as 4 Å in the main-chain and 7.5 Å in the side-chain atoms (Smith *et al*., 1986). Other, smaller, pocket-binding compounds cause similar conformational changes (the root-mean-square difference between the backbone atoms of HRV14·WIN52084s and HRV14 complexed with a smaller compound is less than 0.4 Å), but stabilize the capsid against high temperatures to a lesser extent than the larger WIN compounds (Bibler-Muckelbauer *et al*., 1994). In crystallographic studies the binding site occupancy is only 50 to 60% (Badger *et al*., 1989) after the crystals were equilibrated against 28 μM WIN (Smith *et al*., 1986). In contrast, the minimum inhibitory concentration of WIN52084s that reduces cell plaque counts by a half is 0.03 μM (Rossmann, 1990). Together these factors suggest that inhibition of uncoating occurs without full occupancy of the drug-binding sites. Understanding drug-enhanced stability may require addressing the question of how capsids are stabilized with only fractional occupancy.

Given that filling the pocket with a WIN compound can arrest the viral life cycle at the uncoating step (Fox *et al*., 1986; Pevear *et al*., 1989), it may be proposed that a certain structural flexibility of the pocket is required for the disassembly of the viral capsid. A series of molecular dynamics trajectories were calculated to investigate the influence of WIN compounds on the structural flexibility and dynamic properties of solvated HRV14 and HRV14·WIN52084s. This communication highlights the effect of WIN52084s on the structural flexibility as described by the isothermal compressibility, β_T, estimated from the simulations. The computational results indicate that solvated HRV14·WIN52084s has a greater compressibility than solvated HRV14, counterintuitive to what might be expected for binding a ligand in an internal pocket. However, these results are indeed consistent with an increase in structural stability according to the empirical relationship between β_T and structural stability in proteins first recognized by others (Gekko & Hasegawa, 1986), and provide an insight into the mechanism of the antiviral activity of inhibition of uncoating. We propose that the antiviral activity derives from an entropic stabilization of the capsid, rather than a

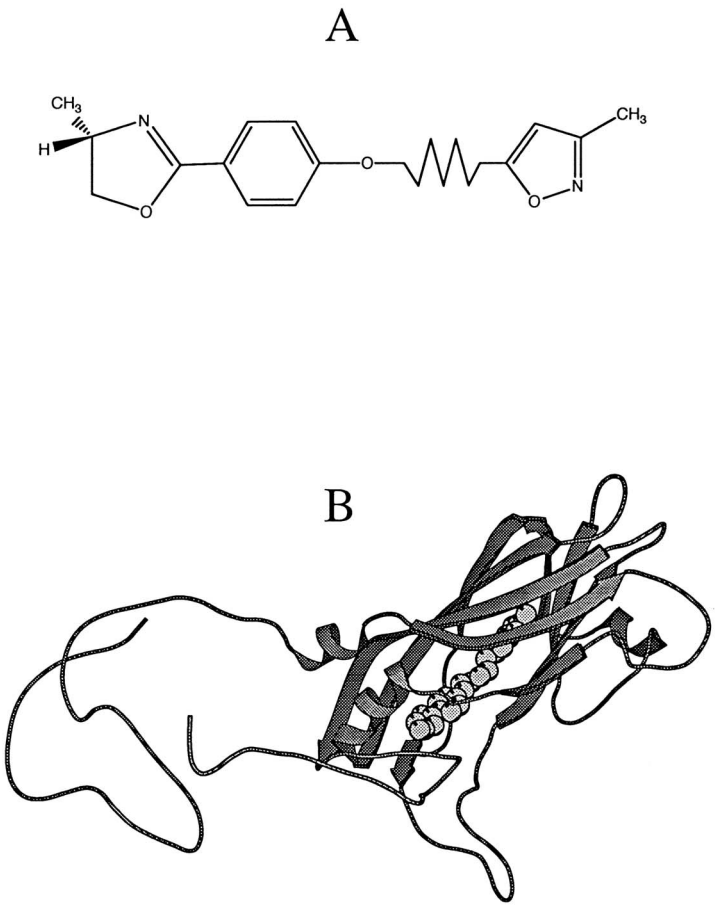

Figure 1. A, The chemical structure of the antiviral compound WIN52084s. Chirality is specified for the methyl group of the oxazoline ring. B, MOLSCRIPT (Kraulis, 1991) ribbon drawing of VP1 with a space-filling model of WIN52084s.

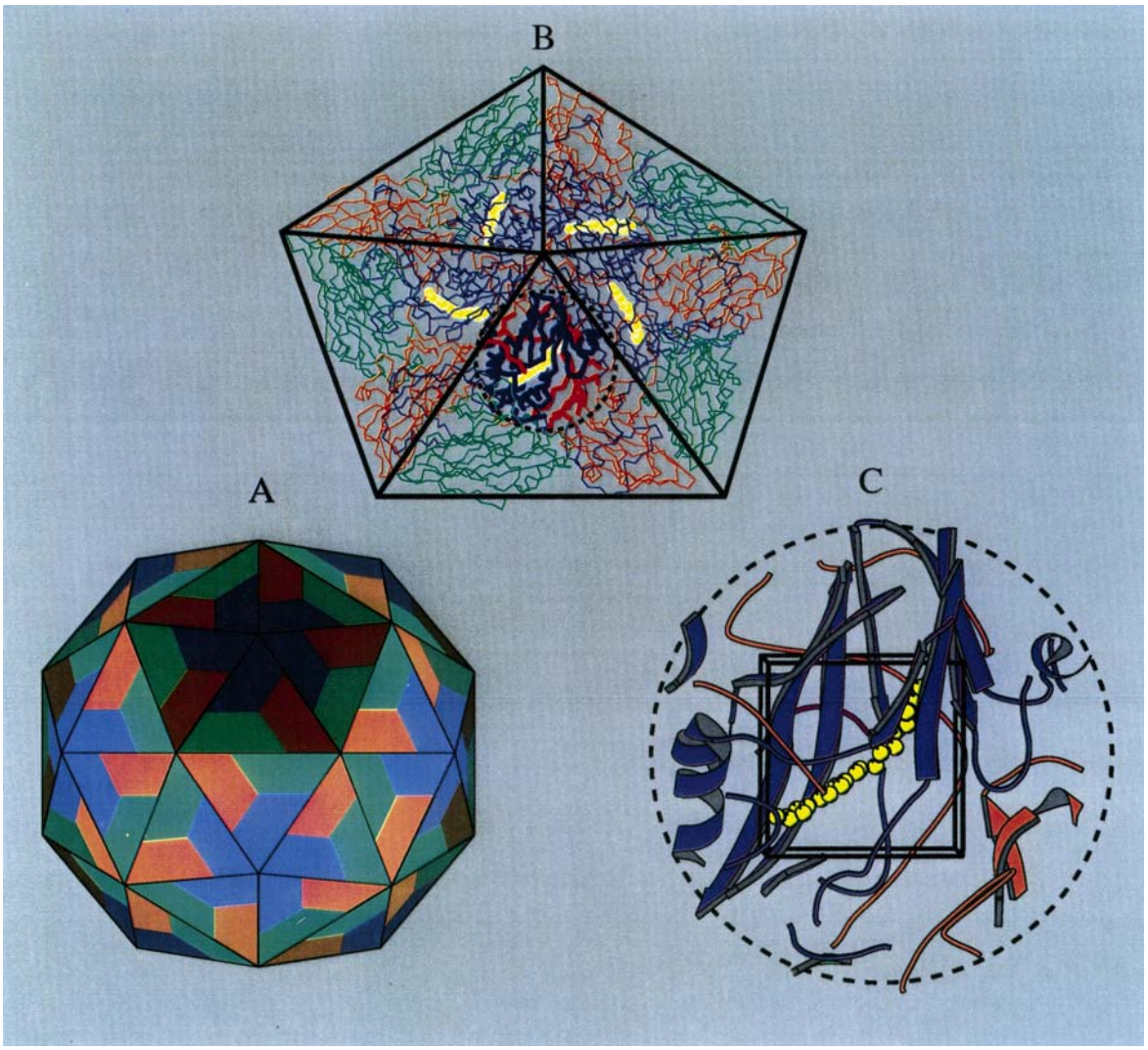

Figure 2. A, Schematic drawing of the HRV14 icosahedral capsid. Colors indicate viral proteins; VP1, blue; VP2, green; VP3, red. B, MOLSCRIPT (Kraulis, 1991) trace of the highlighted pentamer in A of the Cα vectors of VP1, VP2 and VP3. WIN52084s is shown in yellow. C, MOLSCRIPT (Kraulis, 1991) drawing of the spherical SBMD simulation region. Colors as in B, plus VP4, purple. The box shows the region used for the density fluctuation calculations.

The stochastic boundary molecular dynamics (SMBD) method was applied to the spherical region of the virus shown in part C as described in detail by Brooks and Karplus (1989). The simulations were carried out using the CHARMM macromolecular mechanics program (Brooks *et al*., 1983) version 22. The CHARMM version 19 polar hydrogen parameter set was used; with these parameters only hydrogen atoms that can form hydrogen bonds are explicitly included, other hydrogen atoms are implicitly modelled as extended heavy atoms. The TIP3 model represents water. The parameters for WIN52084s were slightly modified from those of Lybrand & McCammon (1988); details of the modifications are contained in a forthcoming paper on these simulations. The water and the explicit hydrogen-heavy atom bonds were fixed using SHAKE (Ryckaert *et al*., 1977). Three 800 ps trajectories were calculated for both solvated HRV14 and solvated HRV14·WIN52084s.

The SMBD method is used to efficiently model the dynamics of large systems by focusing on the region of interest. Rather than follow the trajectories of all virus coat protein atoms (with more than 50,000 residues in all) the system is spatially subdivided into reaction, buffer and reservoir regions. The reaction region (so named because it often includes the active site of an enzyme) here is a 20 Å radius sphere centered about the drug-binding pocket, and where Newtonian dynamics determines the atomic trajectories. The buffer region, a radial shell extending from 20 to 22 Å from the center of the reaction region, acts as a transition between the reaction and reservoir regions. Buffer atoms are propagated by Langevin dynamics. Reservoir region atoms are removed and their influence on the system is mimicked by stochastic forces applied to the buffer atoms. Harmonic constraints referenced to the X-ray coordinates are applied to protein atoms in the buffer region and thus help to maintain the structural integrity of the system. The harmonic constraints for protein atoms and friction coefficients for non-hydrogen atoms in the buffer region are implemented as described by Brooks & Karplus (1989). Finally, the X-ray structure is overlayed with equilibrated boxes of water molecules to eliminate water-sized holes in the simulation sphere. A deformable stochastic boundary applies a rapidly increasing force to water molecules beyond a 22 Å radius (Brooks & Karplus, 1983). After overlaying, the system is energy minimized with the protein atoms fixed to their X-ray coordinates. Then the entire system is energy minimized and an equilibration and heating period of 100 ps initiated. The time step is 0.001 ps, and the target temperature is 300 K. The data collection period is 800 ps during which time the temperature remains constant at 297($\pm$6) K for all simulations. In addition, the total energy of the system remains stable for all simulations (standard deviation in fluctuations is less than 1%).

The 22 Å radius sphere is sufficiently large for the same protein atoms (a total of 2300 atoms), with identical harmonic force constants, to be present in the drug-free and drug-bound simulations. The presence of WIN results in fewer water molecules in the drug-bound virus simulation, but otherwise the drug-free and drug-bound systems have been made as identical as possible.

loss of structural flexibility that kinetically hinders disassembly.

For computational efficiency in this initial study, a stochastic boundary molecular dynamics (SBMD) method (Brooks *et al*., 1985) was used to simulate a 22 Å spherical region centered at the pocket (shown in Figure 2C). With the SBMD method, the positions of a subset of approximately 2500 atoms are propagated by Newtonian dynamics, while those of 700 atoms at the boundary layer of the sphere are propagated by Langevin dynamics to account for the remainder of the system in a continuum sense (see the legend to Figure 2).

Density fluctuations may be related to a macroscopic thermodynamic quantity, the isothermal compressibility, β_T, by the following equation (Reif, 1965):

$$\beta_T = \frac{\overline{(\Delta\rho)^2}V}{\tilde{\rho}^2 kT} \qquad (1)$$

where ρ is the particle density N/V, with N the particle number and V the fixed volume, $\tilde{\rho}$ is the equilibrium particle density, $\overline{(\Delta\rho)^2}$ is the mean square fluctuation in particle density about $\tilde{\rho}$, k is Boltzmann's constant, and T is the absolute temperature. Density fluctuations, typically considered with grand canonical ensembles, can also be evaluated for an open portion of a larger system, as done here. The density is calculated by overlaying a regular array of grid points on the region of interest (Figure 2C) and finding the fraction of points which are inside the van der Waals radii of any protein, solvent, or WIN52084s atom present. As such, for computational convenience, ρ is given as a fractional density rather than the number of atoms per unit volume. The variance of the number density was calculated for time frames saved every 100 fs over the 0.8 ns trajectory. The calculated compressibilities are given in Table 1, along with the fractional equilibrium densities. In recognition of the possible influence from the solvent boundary model on simulated compressibilities, we considered three types of solvation boundary conditions.

A comparison of the corresponding free virus and WIN-bound virus simulations from Table 1 shows that in every case HRV14·WIN52084s has a larger compressibility than HRV14, with the compressibilities ranging from 7×10^{-6} to 15×10^{-6} bar^{-1}. Although experimental compressibilities include effects from protein hydration, the calculated intrinsic compressibilities are very close to experimentally determined values which range from 1×10^{-6} to 15×10^{-6} bar^{-1} for globular proteins. These results are also of comparable magnitude to those obtained by Kitchen *et al*. (1992) when they calculated β_T for bovine pancreatic trypsin inhibitor with constant pressure simulations. An increase of 50% or greater by binding a small ligand representing only about 1% of the overall protein mass has precedent; Fidy *et al*. (1992) measured the compressibility of horseradish peroxidase (HRP) with and without a small hydrophobic molecule bound near the peroxidase heme by an optical hole-burning technique. The presence of this small hydrophobic molecule increases the compressibility of HRP by a factor of 3. The trend of increased compressibility with increased hydrophobicity is not limited to HRP; it is generally found that systems characterized by weaker molecular interactions have larger compressibilities than those with stronger dipolar interactions (Weber & Drickamer, 1983). The molecular dynamics simulation results of Kitchen *et al*. (1992) show the greater compressibilities of water-hydrating nonpolar groups and the lower compressibilities of water-solvating charged groups.

How the change in compressibility upon binding WIN compounds relates to the antiviral activity is seen from a correlation recognized by Gekko and Hasegawa (1986); proteins with larger compressibilities have higher thermal denaturation points, T_m (Figure 3). The data in Figure 3 demonstrate a trend of increasing T_m with increasing β_T, suggesting that, in the case of HRV14, the inhibition of uncoating in the presence of WIN compounds is due to stabilization from a greater compressibility. Following the trend in Figure 3, the increases in β_T shown

Table 1. Calculated isothermal compressibilities and fractional equilibrium densities

	HRV14		HRV14·WIN52084s		HRV14·pWIN52084s	
Solvation[a]	fractional density[b] $\tilde{\rho}$	β_T[c] /(10^{-6} bar^{-1})	fractional density[b] $\tilde{\rho}$	β_T[c] /(10^{-6} bar^{-1})	fractional density[b] $\tilde{\rho}$	β_T[c] /(10^{-6} bar^{-1})
22 Å boundary (359, 309)	0.821	8.9	0.785	11.8		
22 Å boundary (416, 375)	0.818	7.1	0.792	9.3	0.810	7.3
∞ boundary (416, 375)	0.789	10.4	0.755	15.4	0.814	13.4

[a] The boundary potential is repulsive at radial distances greater than that indicated from the SBMD active site center. The total number of water molecules in the simulation is given in parentheses. The first number corresponds to HRV14 and the second number to either HRV14·WIN52084s or HRV14·pWIN52084s. Note that only a fraction of this number is within the box shown in Figure 2C which primarily contains protein or protein and WIN atoms.

[b] $\tilde{\rho}$ is the average fractional density from the 0.8 ns trajectory.

[c] Isothermal compressibility calculated from equation (1) using the standard deviation in the density. The most appropriate direct comparisons are among simulations in the same row that have the same solvation conditions. The densities are calculated from 8000 trajectory points taken every 100 fs using an 18 Å × 18 Å × 10 Å grid with a spacing of 0.2 Å (shown in Figure 2C). It is determined whether a grid point is inside or outside the van der Waals radius of protein, WIN, or H_2O atoms, and the fraction of points within these radii gives the density for a given coordinate set. The results were verified with a smaller grid spacing (0.1 Å) and by increasing the box size by as much as 50%.

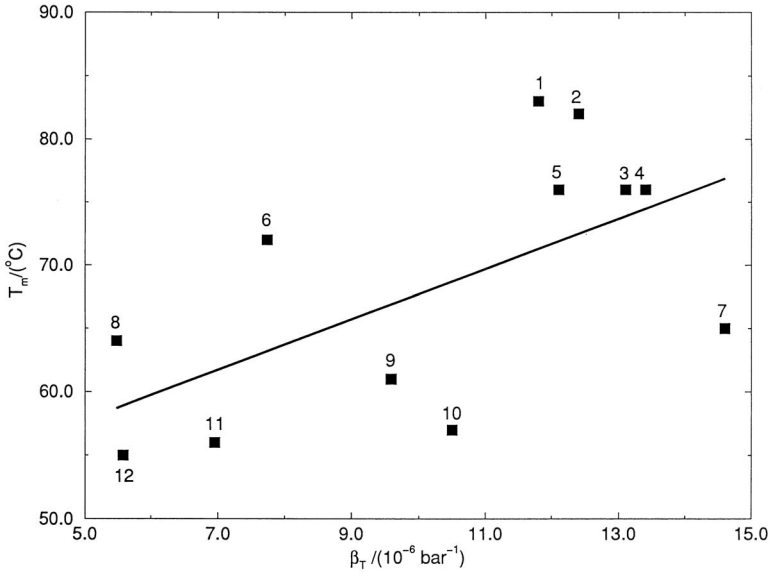

Figure 3. The thermal denaturation temperature of several proteins is plotted as a function of isothermal compressibility, β_T. The proteins designated above are: 1, β-lactoglobulin (bovine)[a]; 2, α-lactalbumin (bovine)[a]; 3, myoglobin (whale)[a,b]; 4, insulin (bovine)[b]; 5, ovalbumin (egg)[a]; 6, lysozyme (egg white)[a,b]; 7, serum albumin (bovine)[a,b]; 8, ribonuclease A (bovine)[b]; 9, catalase (bovine)[a]; 10, carbonic anhydrase (bovine)[a]; 11, α-chymotrypsinogen A (bovine)[a]; 12, trypsinogen (bovine)[b]. Hemoglobin, which is used in the similar figure of Gekko & Hasegawa (1986), is not used here because they use T_m from bovine hemoglobin and β_T from human hemoglobin. In addition, conalbumin was excluded due to the high heating rate used by Donovan *et al.* (1975) to obtain T_m. All β_T values are from Gekko & Hawegawa (1986) and T_m values from either [a]Stellwagen & Wilgus (1978) or [b]Bull & Breese (1973). The regression coefficient for the continuous line is 0.61.

in Table 1 would correspond to an increase in T_m of approximately 5 to 12 deg. C.

Why should greater compressibility correlate with enhanced thermal stability? Increased compressibility suggests a greater accessible conformational space and larger entropy of HRV14·WIN52084s relative to HRV14. This suggestion is born out by the compilation from the literature shown in Figure 4 for the entropies of unfolding per residue at 25°C *versus* compressibility for several proteins. The value ΔS_N^D diminishes for proteins of greater β_T. If the entropy per residue in the unfolded state is assumed to be constant, the smaller difference between the denatured and native states means the entropy in the folded state increases with the compressibility.

The variation in compressibility for these groups may be rationalized on the basis of the nature of intermolecular interactions. To do so, consider the relationship between the free energy of the system and the compressibility, or density fluctuations (see equation (1)). Following the discussion of Reif (1965), for $\mathscr{P}(N)\,dN$, the probability that the particle number of a system† is between N and $N + \mathrm{d}N$ is:

$$\mathscr{P}(N)\,\mathrm{d}N \propto \exp\left[-\frac{G_0(N)}{kT}\right]\mathrm{d}N \qquad (2)$$

where $G_0(N)$ is the free energy with particle number N. Fluctuations about the free energy minimum, $G_{\min}$, can be expanded:

$$G_0 - G_{\min} = \left(\frac{\partial G_0}{\partial N}\right)_T \Delta N + \frac{1}{2}\left(\frac{\partial^2 G_0}{\partial N^2}\right)_T (\Delta N)^2 + \cdots \qquad (3)$$

† The discussion here is in terms of fluctuations in the particle number since this quantity is calculated from the simulations. However, a discussion in terms of volume fluctuations is equivalent.

with $\Delta N = N - \tilde{N}$, where $\tilde{N}$ is the particle number at $G_{\min}$. At equilibrium, the free energy, G_0, is stationary, therefore $(\partial G_0/\partial N)_T = 0$. Also, we have from standard thermodynamics (Hill, 1994):

$$\left(\frac{\partial^2 G_0}{\partial N^2}\right)_T = -\frac{V^2}{N^2}\left(\frac{\partial P}{\partial V}\right)_{T,N} \qquad (4)$$

where P is the pressure. Recalling the thermodynamic definition of the isothermal compressibility, $\beta_T = -1/V\,(\partial V/\partial P)_T$, this gives us:

$$\left(\frac{\partial^2 G_0}{\partial \tilde{N}^2}\right)_T = \frac{V}{\tilde{N}^2\beta_T}. \qquad (5)$$

Thus, for small ΔN equation (3) becomes:

$$G_0(N) = G_{min} + \frac{(\Delta N)^2 V}{2\tilde{N}^2\beta_T} \qquad (6)$$

Combining equation (6) and equation (2) and collecting constants into B yields:

$$\mathscr{P}(N)\,\mathrm{d}N = B\exp\left[-\frac{(\Delta N)^2 V}{2kT\tilde{N}^2\beta_T}\right] \qquad (7)$$

Therefore the variance in particle number is:

$$\overline{(\Delta N)^2} = \frac{kT\tilde{N}^2\beta_T}{V} \qquad (8)$$

which at constant V gives equation (1).

Two points should be noted from the relationship between free energy and compressibility apparent in equations (5), (6) and (7). Firstly, changes in compressibility, as a general principle, involve changes in the curvature of G_0 as given by $(\partial^2 G_0/\partial N^2)_T$, and secondly, are not related to relative levels of free energy as given by $G_{\min}$. Thus, β_T does not reflect the value of $G_{\min}$, but the curvature of the free energy surface; a smoother free energy surface,

with weaker forces of interaction, corresponds to greater compressibilities and larger density fluctuations.

We examined the response of β_T estimated from the simulations to a change in the nature of the free energy surface by the use of a hypothetical ''polar'' WIN52084s named pWIN52084s. pWIN52084s is the same as WIN52084s except that the parameters for the most hydrophobic atoms have been changed so that they have a charge either 0.5 more or 0.5 less than the unmodified WIN52084s parameters while maintaining charge neutrality. This hypothetical pWIN52084s has a polarity more similar to the six to eight water molecules present in the wild-type HRV14 pocket than a hydrophobic WIN52084s. Results from 800 ps SBMD simulations with pWIN52084s (Table 1) yield compressibilities lower than WIN-bound simulations but somewhat greater than the drug-free simulations. The ordering of compressibilities of HRV14·WIN52084s > HRV14·pWIN52084s $\geqslant$ HRV14·(pocket water), while the ordering in strength of intermolecular interactions is HRV14·WIN52084s < HRV14·pWIN52084s and HRV14·WIN52084s < HRV14·(pocket water). Because β_T reflects the strength of intermolecular interactions the difference in compressibility between WIN-bound and WIN-free rhinovirus is not a consequence of the difference in protein structure.

Additional evidence that the stabilization of HRV14 does not arise from conformational changes in VP1 comes from the drug-fragment studies of Bibler-Muckelbauer *et al*. (1994). They have found that the conformational changes associated with drug fragments are very similar to those found for larger drugs, but that the thermal stabilization is not as good. Consequently, the conformational change alone does not appear to be sufficient to enhance capsid stability significantly. This is consistent with the conclusion suggested by pWIN and the compressibility-stability relationship that we postulate; the protein structure in the pWIN simulations are nearly identical to those for normal WIN but the compressibility differs significantly.

We have described here an increase in the compressibility of drug-bound rhinovirus over that of drug-free virus and have proposed that this increased compressibility is related to greater thermal stability *via* an increase in the conformational entropy of the drug-bound virus. Earlier work on viruses (Lauffer *et al*., 1958, Prevelige *et al*., 1994, Da Poian *et al*., 1995) has shown that there is a strong entropic driving force in the assembly of these viruses. However, we note that these authors interpret the entropy change to result from the release of water molecules from apolar side-chains and the consequent exchange of water-protein interactions for weaker protein-protein interactions. This basis for entropic stabilization (suggested by these authors) differs from the change in protein conformational entropy described here. The increase in conformational entropy with drug binding has the virtue of helping to rationalize the efficacy of the drug with less than full occupancy. With this increase in entropy there is a greater density of conformational states for the deposition of thermal energy, leading to enhanced stability when only a few sites are occupied. Moreover, since both subunit-subunit contacts and tertiary structure interactions are present in the simulation system, the observed effects on compressibility may be relevant to either the dissociation or unfolding of subunits during the disassembly process. Thermodynamics gives no simple proportionality between S and β_T, thus the relationship shown in Figure 4 may be particular to proteins. The results presented here suggest that compressibility is a fundamental property significant for understanding antiviral activity and uncoating that should be considered in examinations of viral capsid structural stability and disassembly.

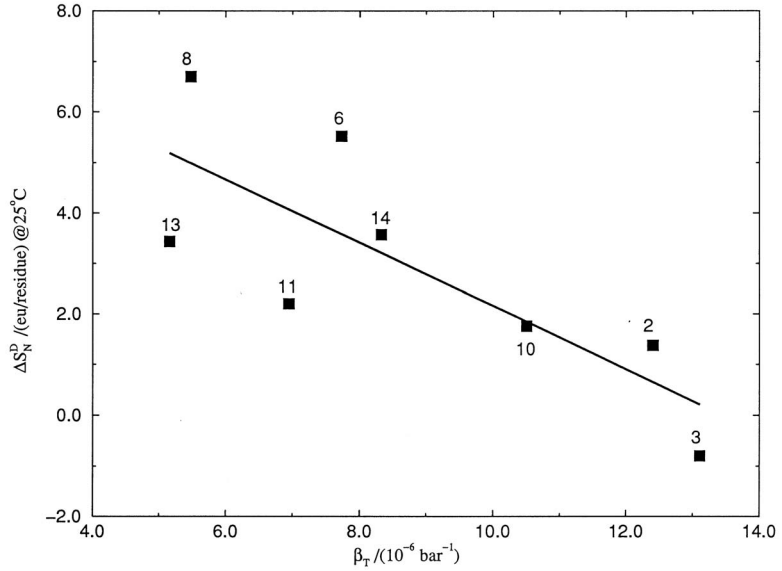

Figure 4. Proteins are numbered as in Figure 3, plus 13, trypsin and 14, α-chymotrypsin. ΔS_N^D is the change in entropy per residue for the transition of the native (N) to the denatured (D) state at 25°C. Entropy data are from Table I of Privalov & Gill (1988), except for chymotrypsinogen (Brandts, 1964) and α-lactalbumin (Xie *et al*., 1991). All β_T values are from Gekko & Hasegawa (1986). The regression coefficient for the continuous line is –0.79.

Acknowledgements

We thank Profs Igal Szleifer and Ron Levy for valuable discussions and Prof Ron Levy for suggesting the study of a polar WIN compound. This work was supported by the Lucille P. Markey foundation and an SUR grant from IBM.

References

Badger, J., Minor, I., Kremer, M. J., Oliveira, M. A., Smith, T. J., Griffith, J. P., Guerin, D. M. A., Krishnaswamy, S., Luo, M., Rossmann, M. G., McKinlay, M. A., Diana, G. D., Dutko, F. J., Fancher, M., Rueckert, R. R. & Heinz, B. A. (1988). Structural analysis of a series of antiviral agents complexed with human rhinovirus 14. *Proc. Natl Acad. Sci. USA*, **85**, 3304–3308.

Badger, J., Minor, I., Oliveira, M. A., Smith, T. J. & Rossmann, M. G. (1989). Structural analysis of antiviral agents that interact with the capsid of human rhinoviruses. *Proteins: Struct. Funct. Genet.* **6**, 1–19.

Bibler-Muckelbauer, J. K., Kremer, M. J., Rossmann, M. G., Diana, G. D., Dutko, F. J., Pevear, D. C. & McKinlay, M. A. (1994). Human rhinovirus 14 complexed with fragments of active antiviral compounds. *Virology*, **202**, 360–369.

Brandts, J. F. (1964). The thermodynamics of protein denaturation. 1. The denaturation of chymotrypsinogen. *J. Am. Chem. Soc.* **86**, 4291–4301.

Brooks, B. R., Bruccoleri, R. E., Olafson, B. D., States, D. J., Swaminathan, S. & Karplus, M. (1983). CHARMM: a program for macromolecular energy, minimization, and dynamics calculations. *J. Comput. Chem.* **4**, 187–217.

Brooks, C. L., III & Karplus, M. (1983). Deformable stochastic boundaries in molecular dynamics. *J. Chem. Phys.* **79**, 6312–6325.

Brooks, C. L., III & Karplus, M. (1989). Solvent effects on protein motion and protein effects on solvent motion: dynamics of the active site region of lysozyme. *J. Mol. Biol.* **208**, 159–181.

Brooks, C. L., III, Brunger, A. & Karplus, M. (1985). Active site dynamics in protein molecules: a stochastic boundary molecular-dynamics approach. *Biopolymers*, **24**, 843–865.

Bull, H. B. & Breese, K. (1973). Thermal stability of proteins. *Arch. Biochem. Biophys.* **158**, 681–686.

Da Poian, A. T., Oliveira, A. C. & Silva, J. L. (1995). Cold denaturation of an icosahedral virus. The role of entropy in virus assembly. *Biochemistry*, **34**, 2672–2677.

Donovan, J. W., Mapes, C. J., Davis, J. G. & Garibaldi, J. A. (1975). A differential scanning calorimetric study of the stability of egg white to heat denaturation. *J. Sci. Fd. Agri.* **26**, 73–83.

Fidy, J., Vanderkooi, J. M., Zollfrank, J. & Friedrich, J. (1992). Softening of the packing density of horseradish peroxidase by a H-donor bound near the heme pocket. *Biophys. J.* **63**, 1605–1612.

Filman, D. J., Rashid, S., Chow, M., Macadam, A. J., Minor, P. D. & Hogle, J. M. (1989). Structural factors that control conformational transitions and serotype specificity in type 3 poliovirus. *EMBO J.* **8**, 1567–1579.

Fox, M. P., Otto, M. J. & McKinlay, M. A. (1986). The prevention of rhinovirus and poliovirus uncoating by WIN 51711: a new antiviral drug. *Antimicrob. Agents Chemother.* **30**, 110–116.

Gekko, K. & Hasegawa, Y. (1986). Compressibility-structure relationship of globular proteins. *Biochemistry*, **25**, 6563–6571.

Grant, R. A., Hiremath, C. N., Filman, D. J., Syed, R., Andries, K. & Hogle, J. M. (1994). Structures of poliovirus complexes with anti-viral drugs: implications for viral stability and drug design. *Curr. Biol.* **4**, 784–797.

Heinz, B. A., Rueckert, R. R., Shepard, D. A., Dutko, F. J., McKinlay, M. A., Fancher, M., Rossmann, M. G., Badger, J. & Smith, T. J. (1989). Genetic and molecular analyses of spontaneous mutants of human rhinovirus 14 that are resistant to an antiviral compound. *J. Virol.* **63**, 2476–2485.

Heinz, B. A., Shepard, D. A. & Rueckert, R. R. (1990). Escape mutant analysis of a drug-binding site can be used to map functions in the rhinovirus capsid. In *Use of X-Ray Crystallography in the Design of Antiviral Agents* (Laver, W. G. & Air, G. M., eds), pp. 173–186, Academic Press, San Diego, CA.

Hill, T. L. (1994). *Thermodynamics of Small Systems*, part 2, pp. 59–60. Dover Publications Inc., New York.

Kitchen, D. B., Reed, L. H. & Levy, R. M. (1992). Molecular dynamics simulation of solvated protein at high pressure. *Biochemistry*, **31**, 10083–10093.

Kraulis, P. J. (1991). MOLSCRIPT: a program to produce both detailed and schematic plots of protein structures. *J. Appl. Crystallog.* **24**, 946–950.

Lauffer, M. A., Ansevin, A. T., Cartwright, T. E. & Brinton, C. C. (1958). Polymerization-depolymerization of tobacco mosaic virus protein. *Nature*, **181**, 1338–1339.

Lybrand, T. P. & McCammon, J. A. (1988). Computer simulation study of the binding of an antiviral agent to a sensitive and resistant human rhinovirus. *J. Comput. Aided Mol. Design*, **2**, 259–266.

Pevear, D. C., Fancher, M. J., Felock, P. J., Rossmann, M. G., Miller, M. S., Diana, G., Treasurywala, A. M., McKinlay, M. A. & Dutko, F. J. (1989). Conformational change in the floor of the human rhinovirus canyon blocks adsorption to HeLa cell receptors. *J. Virol.* **63**, 2002–2007.

Prevelige, P. E., King, J. & Silva, J. L. (1994). Pressure denaturation of the bacteriophage P22 coat protein and its entropic stabilization in icosahedral shells. *Biophys. J.* **66**, 1631–1641.

Privalov, P. L. & Gill, S. J. (1988). Stability of protein structure and hydrophobic interaction. *Advan. Protein Chem.* **39**, 191–234.

Reif, F. (1965). *Fundamentals of Statistical and Thermal Physics*, McGraw-Hill Book Company.

Rossmann, M. G. (1990). Neutralizing rhinoviruses with antiviral agents that inhibit attachment and uncoating. In *Use of X-Ray Crystallography in the Design of Antiviral Agents* (Laver, W. G. & Air, G. M., eds), pp. 115–137, Academic Press, San Diego, CA.

Rossmann, M. G. (1994). Viral cell recognition and entry. *Protein Sci.* **3**, 1712–1725.

Rossmann, M. G., Arnold, E., Erickson, J. W., Frankenberger, E. A., Griffith, J. P., Hecht, H. J., Johnson, J. E., Kamer, G., Luo, M., Mosser, A. G., Rueckert, R. R., Sherry, B. & Vriend, G. (1985). Structure of a human cold virus and functional relationship to other picornaviruses. *Nature*, **317**, 145–153.

Ryckaert, J.-P., Ciccotti, G. & Berendsen, H. J. C. (1977). Numerical integration of the cartesian equations of motion of a system with constraints:

molecular dynamics of n-alkanes. *J. Comput. Phys.* **23**, 327–341.

Smith, T. J., Kremer, M. J., Luo, M., Vriend, G., Arnold, E., Kamer, G., Rossmann, M. G., McKinlay, M. A., Diana, G. D. & Otto, M. J. (1986). The site of attachment of human rhinovirus 14 for antiviral agents that inhibit uncoating. *Science*, **233**, 1286–1293.

Stellwagen, E. & Wilgus, H. (1978). Relationship of protein thermostability to accessible surface area. *Nature*, **275**, 342–343.

Weber, G. & Drickamer, H. G. (1983). The effect of high pressure upon proteins and other biomolecules. *Quart. Rev. Biophys.* **16**, 89–112.

Xie, D., Bhakuni, V. & Freire, E. (1991). Calorimetric determination of the energetics of the molten globule intermediate in protein folding: apo-α-lactalbumin. *Biochemistry*, **30**, 10673–10678.

Edited by B. Honig

(Received 20 June 1995; accepted 13 September 1993)

Note added in proof: After acceptance of this paper we became aware of an article (Gerstein *et al.*, 1995, *J. Mol. Biol.* **249**, 955–966) relating to calculation of volume fluctuations of proteins using Voroni polyhedra.